Epithelial basement membrane injury and regeneration modulates corneal fibrosis after pseudomonas corneal ulcers in rabbits

Gustavo K. Marino[a,b], **Marcony R. Santhiago**[b], **Abirami Santhanam**[a], **Luciana L. Dibbin**[a], **Shanmugapriya Thangavadivel**[a], **Carla S. Medeiros**[a], **Karthikeyan Bose**[a], **Kwai Ping Tam**[a], and **Steven E. Wilson**[a,*]

[a]Cole Eye Institute, Cleveland Clinic, Cleveland, Ohio

[b]University of São Paulo, São Paulo, Brazil

Abstract

The purpose of this study was to investigate whether myofibroblast-related fibrosis (scarring) after microbial keratitis was modulated by the epithelial basement membrane (EBM) injury and regeneration. Rabbits were infected with *Pseudomonas aeruginosa* after epithelial scrape injury and the resultant severe keratitis was treated with topical tobramycin. Corneas were analyzed from one to four months after keratitis with slit lamp photos, immunohistochemistry for alpha-smooth muscle actin (α-SMA) and monocyte lineage marker CD11b, and transmission electron microscopy. At one month after keratitis, corneas had no detectable EBM lamina lucida or lamina densa, and the central stroma was packed with myofibroblasts that in some eyes extended to the posterior corneal surface with damage to Descemet's membrane and the endothelium. At one month, a nest of stromal cells in the midst of the SMA+ myofibroblasts in the stroma that were CD11b+ may be fibrocyte precursors to myofibroblasts. At two to four months after keratitis, the EBM fully-regenerated and myofibroblasts disappeared from the anterior 60 to 90% of the stroma of all corneas, except for one four-month post-keratitis cornea where anterior myofibroblasts were still present in one localized pocket in the cornea. The organization of the stromal extracellular matrix also became less disorganized from two to four months after keratitis but remained abnormal compared to controls at the last time point. Myofibroblasts persisted in the posterior 10% to 20% of posterior stroma even at four months after keratitis in the central cornea where Descemet's membrane and the endothelium were damaged. This study suggests that the EBM has a critical role in modulating myofibroblast development and fibrosis after keratitis—similar to the role of EBM in fibrosis after photorefractive keratectomy. Damage to EBM likely allows epithelium-derived transforming growth factor beta (TGFβ) to penetrate the stroma and drive development and persistence of myofibroblasts. Eventual repair of EBM leads to myofibroblast

Corresponding Author: Steven E. Wilson, MD, Cole Eye Institute, I-32, Cleveland Clinic, 9500 Euclid Ave, Cleveland, OH, United States. wilsons4@ccf.org.

Proprietary interest statement: None of the authors have any commercial or proprietary interest in this study.

apoptosis when the cells are deprived of requisite TGFβ to maintain viability. The endothelium and Descemet's membrane may serve a similar function modulating TGFβ penetration into the posterior stroma—with the source of TGFβ likely being the aqueous humor.

Keywords

Stromal fibrosis (scarring) commonly occurs after bacterial keratitis and often causes severe loss in visual function (Gopinathan et al., 2009). Regeneration of the epithelial basement membrane (EBM) is a key determinant of regenerative (transparent) versus fibrotic (scarred) corneal healing after photorefractive keratectomy (Torricelli et al., 2013a; Torricelli et al., 2013b; Torricelli et al., 2016). The structural and functional regeneration of the EBM is critical because of its important function in regulating the bidirectional passage of cytokines, chemokines and growth factors—including transforming growth factor (TGF) β and platelet-derived growth factor (PDGF), between the epithelium or the tear film and the stroma—where TGFβ and PDGF regulate the development and persistence of fibrosis-associated myofibroblasts from precursor cells (Singh et al., 2011). Myofibroblasts produce fibrosis (scarring) of the corneal stroma because they are opaque due to diminished crystallin protein production relative to keratocytes (Jester et al., 1999) and they secrete disordered extracellular matrix that alters the precise distribution of the collagen fibers that is essential for corneal transparency (Hassell and Birk, 2010). The aim of the present study was to determine 1) whether corneal stromal fibrosis that occurs after a severe bacterial corneal ulcer is associated with EBM injury and 2) whether eventual EBM regeneration is associated with the disappearance of stromal myofibroblasts.

All animals were treated in accordance with the tenets of the ARVO Statement for the Use of Animals in Ophthalmic and Vision Research. The Animal Control Committee and Institutional Biosafety Committee at the Cleveland Clinic approved this animal study.

Twelve- to 15-week-old female New Zealand white rabbits weighing 2.5 to 3.0 kg each were included in this study. General anesthesia was obtained by intramuscular injection of ketamine hydrochloride (30 mg/kg) and xylazine hydrochloride (5 mg/kg). In addition, topical proparacaine hydrochloride 0.5% (Akorn Inc., Lake Forest, IL) was applied to both eyes at the time of the procedure. Rabbits were also treated with acetaminophen 20 mg per 100 ml of drinking water for five days after infection and buprenorphine 0.05 mg/kg by subcutaneous injection twice a day for up to 10 days after infection, as needed if there were signs of discomfort.

One eye was randomly selected to be infected, while the opposite eye was included as an uninfected control. A wire lid speculum was positioned in the eye followed by the production of a small central epithelial defect with a #64 Beaver blade (BD Beaver, Waltham, MA). The epithelial defect was inoculated with *Pseudomonas aeruginosa* (Hazlett, 2007; Fleiszig and Evans, 2002) at a concentration of 20 CFU/μL in balanced salt solution. The strain of bacteria used named PA3346 and was a clinical isolate from a patient with a

corneal ulcer that was highly sensitive to tobramycin. The strain was genotyped for ExoS, ExoU, ExoT and ExoY using previously published PCR primers and methods (Ledbetter et al., 2009) and was found to be ExoS+, ExoT+ and ExoY+, and ExoU-.

The eyes were monitored untreated for 24–36 hours until severe keratitis developed (Fig. 1A) and then were treated with topical 13.5 mg/ml tobramycin (Sigma-Aldrich, St. Louis, MO) every hour for two days and then every two hours for five days. Corticosteroids were not applied to avoid the potential confounding effects on the corneal wound healing response. Epithelial defects in all eyes were found to heal by 7 to 10 days after the initial infection.

Rabbits were anesthetized with ketamine and xylazine for slit lamp photographs and then euthanized with an intravenous injection of 100 mg/kg pentobarbital. The corneoscleral rims of infected and uninfected control eyes were removed without manipulation of the cornea using 0.12 mm forceps and sharp Westcott scissors (Fairfield, CT). The corneas were cut into two equal halves with a sharp straight-edged razor blade and one half was embedded in liquid optimal cutting temperature (OCT) compound (Sakura FineTek, Torrance, CA) within a $24 \times 24 \times 5$ mm mold (Fisher Scientific, Pittsburgh, PA) and quickly frozen on a block of dry ice and stored at $-80°C$ until sectioning was performed for immunohistological evaluation. The second corneal half was immediately stored in 2.5% glutaraldehyde and 4% paraformaldehyde in 0.2 M cacodylate buffer at $4°C$ for transmission electron microscopy (TEM) evaluation. Two ulcer and two uninfected control corneas were analyzed at each time point (one, two, three and four months) after the pseudomonas infection using immunohistochemistry and TEM.

Corneal sections (7 μm thick) were cut within the central cornea pseudomonas infected and uninfected control corneas with a cryostat (HM 505M; Micron GmbH, Walldorf, Germany) and placed on $25 \times 75 \times 1$ mm microscope slides (Superfrost Plus; Fisher Scientific, Pittsburgh, PA) and maintained at $-80°C$ until used for immunohistochemical analysis. Immunohistochemistry was performed (Torricelli et al., 2013b) to detect the alpha-smooth muscle actin (α-SMA) marker for myofibroblasts or the CD11b marker for monocytes. Briefly, for α-SMA a mouse monoclonal anti-human α-SMA clone 1A4 (Cat# M-0851, Dako, Carpinteria, CA) was used as the primary antibody. The slides were washed with PBS and incubated for 90 minutes at room temperature with anti–α-SMA antibody at 1:50 dilution in 1% BSA. Slides were washed twice with phosphate buffered saline (PBS) and then incubated at room temperature with a secondary antibody, Alexa Fluor 568 goat anti-mouse IgG (Cat# A-11004, ThermoFisher Scientific, Rockford, IL) at a dilution of 1:100 in 1% BSA for 1 hour. For CD11b, monoclonal antibody (Cat# MA1-80091, Invitrogen, Thermo-Fisher, Grand Island, NY) was used as the primary antibody. The slides were washed with PBS and incubated for 90 minutes at room temperature with anti-CD11b antibody at 1:25 dilution in 1% BSA. The slides were then washed twice with PBS and incubated at room temperature with secondary goat anti-rat IgG (H+L), Alexa Fluor 488 (Cat# A-11006, Invitrogen (Thermo-Fisher) at 1:100 dilution for 60 minutes. Coverslips were mounted with Vectashield containing 4',6-diamidino-2-phenylindole (DAPI) (Vector Laboratories Inc., Burlingame, CA) to allow visualization of all nuclei in the tissue sections. Negative controls for α-SMA or CD11b included a non-specific antibody of the same

isotype since no antigen was available for pre-absorption. The sections were analyzed and photographed with a Leica DM5000 microscope (Leica, Buffalo Grove, IL) equipped with Q-imaging Retiga 4000RV (Surrey, BC, Canada) camera and Image-Pro software (MediaCybernetics, Inc. Bethesda, MD).

TEM samples were prepared as previously described (Fantes et al., 1990). Briefly, 1 mm wide, full-thickness blocks of central cornea were cut perpendicular to the epithelial surface from both the pseudomonas ulcer and control corneas, and were fixed in the 2.5% glutaraldehyde and 4% paraformaldehyde with 0.2 M cacodylate buffer solution for a minimum of 24 hours. The excised blocks of central corneas were then rinsed with 0.2 M cacodylate buffer three times for five minutes, post-fixed in 1% osmium tetroxide for 60 minutes at 4°C, and dehydrated in increasing concentrations of ethanol from 30% to 95% for 5 minutes each at 4°C. Finally, dehydration was performed using three 10-minute rinses in 100% ethanol at room temperature and three 15-minute rinses with propylene oxide at room temperature. Samples were then embedded in epoxy resin medium. One-micrometer-thick sections were stained with toluidine blue for light microscopy. Ultrathin 85 nm thick sections were cut with a diamond knife and stained with 5% uranyl acetate and lead citrate. Sections were analyzed and photographed using a Philips CM12 transmission electron microscope operated at 60 kV (FEI Company, Hillsboro, OR).

Control corneas had no α-SMA+ myofibroblasts detected by immunohistochemistr166 y analysis (Fig. 2A). TEM of control corneas revealed the normal EBM lamina lucida and lamina densa characteristic of rabbit corneas (Fig. 2B) (Sta Iglesia and Stepp, 2000; Torricelli et al., 2013b).

All pseudomonas-infected corneas healed with closure of the epithelial defects over seven to ten days after infection (no fluorescein staining) and developed dense stromal scarring with vascularization. All eight infected corneas had 4+ stromal scarring at the slit lamp with no view of the iris at one month after infection (Fig. 1B). There was a definite decrease in opacity at the slit lamp in the four corneas that reached three months and the two corneas that reached four-months post infection (Figs. 1C–E), although iris details were still obscured at these time points.

At one month keratitis, immunohistochemistry showed nearly full stromal thickness high density α-SMA+ myofibroblasts in one cornea (Fig. 2C) and full stromal thickness high density α-SMA+ myofibroblasts in the other cornea removed at this time point (not shown). At two months after keratitis, α-SMA+ myofibroblasts had substantially disappeared in the anterior 50 to 60% of the stroma of both corneas removed at this time point (Fig. 2E), but α-SMA+ myofibroblasts were still present at high density in the posterior half of the stroma in both corneas (Fig. 2E). At three (Fig. 2G) and four (Fig. 2I) months after keratitis, there was further disappearance of α-SMA+ myofibroblasts in the anterior to mid stroma, except for residual α-SMA+ myofibroblasts in a less than 0.5mm diameter pocket in the anterior to mid stroma of one four-month cornea, and α-SMA+ cells associated with stromal blood vessels in several corneas from three to four months after keratitis. Most stromal α-SMA+ myofibroblasts that persisted at three and four months after keratitis were confined to the most posterior 10% to 20% of the stroma (Figs. 2G and 2I) in the central cornea where there

was no endothelium present. A collage of the second cornea removed at two months after infection (Fig. 2K) showed no α-SMA+ myofibroblasts in the peripheral cornea where the endothelium and Descemet's membrane were intact, but persistence of α-SMA+ myofibroblasts in the adjacent posterior stroma overlying injured endothelium and Descemet's membrane. α-SMA+ cells were also associated with a blood vessel that extended across central stroma of this cornea (Fig. 2K). Double staining for monocyte marker CD11b and α-SMA+ revealed that at one month after keratitis there was a nest of CD11b+ cells in the midst of the α-SMA+ myofibroblasts (Fig. 2L) that likely are CD11b+ fibrocyte progenitors to myofibroblasts (Abe et al., 2001). At two months after keratitis only a few scattered CD11b+ cells could be detected in the stroma (not shown). At three and four months after keratitis, no CD11b+ cells remained in the stroma even where SMA+ myofibroblasts persisted, except associated with neovascular blood vessels in the stroma (Fig. 2M).

At one month after keratitis, TEM analysis found no evidence of EBM lamina lucida or lamina densa at magnifications of 20,000X and greater, and the stroma was packed with cells having the typical ultrastructure characteristic of myofibroblasts, with large amounts of rough endoplasmic reticulum, in disorganized extracellular matrix (Fig. 2D). At two (Fig. 2F), three (Fig. 2H) and four months (Fig 2J) after the infection, the EBM was fully regenerated with lamina lucida and lamina densa. It's likely there was a localized area in which the EBM was defective where anterior myofibroblasts persisted (Fig. 2M) in a four-months post-keratitis cornea, but TEM could not be performed to confirm this because this portion of that cornea was cryopreserved and, therefore, not suitable for TEM analysis. Few, if any, myofibroblasts were detected in the subepithelial stroma at two or three months after infection (Figs. 2F and 2H) but cells with typical myofibroblast ultrastructure with large amounts of rough endoplasmic reticulum persisted in the posterior 20 to 40% of stroma at two and three months after infection (not shown). At four months after the infection (Fig. 2J), fully-regenerated EBM with lamina lucida and lamina densa was present in the previously infected zone of both corneas (Fig. 2J). Cells with the morphology of myofibroblasts were only detected in posterior 10% to 20% of stroma where no corneal endothelial cells were present and severe damage to Descemet's membrane was noted in all corneas studied from two to four months after keratitis.

The anterior stroma became progressively more organized from two months (Fig. 2F) to three months (Fig. 2H) to four months (Fig. 2J) after keratitis. This correlated with the decrease in scarring noted at the slit lamp at the three- and four-month time points (Figs. 1D and 1E).

This study demonstrates that injury to the EBM after severe *Pseudomonas aeruginosa* keratitis (Hazlett, 2007; Fleiszig and Evans, 2002) leads to myofibroblast development and severe fibrosis that is similar to, but more extensive than, defective EBM-associated fibrosis that occurs after photorefractive keratectomy (PRK) for correction of high myopia in rabbits (Torricelli et al., 2013b; Torricelli et al., 2016). The large numbers of myofibroblasts generated after the severe keratitis likely develop from both bone marrow-derived and keratocyte-derived precursor cells (Barbosa et al., 2010; Singh et al., 2014). Also, similar to the rabbit PRK model (Marino et al., in press), regeneration of normal EBM lamina lucida

and lamina densa at two months to four months after pseudomonas keratitis is associated with the disappearance of anterior stromal α-SMA+ myofibroblasts. We hypothesize that these anterior to mid-stromal myofibroblasts die by apoptosis after normal EBM regenerates and decreases the penetration of epithelium-derived TGFβ and PDGF into the stroma. Subsequently, the stroma is repopulated with keratocytes that may facilitate EBM regeneration through the production of EBM components (Santhanam et al., 2017; Marino et al, in press). Thus, keratocyte contributions of EBM components such as laminin α-3 and nidogen-2 may be critical to the EBM regeneration process following corneal injury (Santhanam et al., 2017). The few α-SMA+ cells that persist in the anterior 50% to 80% of stroma at two through four months after infection (Figs. 2E, 2G and 2I), other than a small pocket of myofibroblasts in one four-month post-keratitis cornea, are probably pericytes in the walls of the invading blood vessels (Bergers and Songa, 2005).

The persistence of α-SMA+ myofibroblasts in the posterior stroma of some corneas at two through four months after severe keratitis (Figs. 2E, 2G and 2I)—when the myofibroblasts in the anterior to mid-stroma have disappeared—is also of great interest. Corneal myofibroblasts require an ongoing source of TGFβ to develop and survive (Singh et al., 2014). In most of the corneas in this study, the central corneal endothelium and Descemet's membrane were damaged by the severe keratitis. In these areas, α-SMA+ myofibroblasts persisted in approximately the posterior 10% of the central stroma. In the peripheral cornea, where the corneal endothelium and Descemet's membrane were not injured, there were no posterior α-SMA+ myofibroblasts. The transition between posterior stroma with myofibroblasts and posterior stroma without myofibroblasts was abrupt (Fig. 2K), and corresponded to damaged endothelium/Descemet's membrane and intact endothelium/ Descemet's membrane, respectively. TGFβ-1 and TGFβ-2 have been detected in the aqueous humor (Granstein et al., 1990; Cousins et al., 1991). Likely, the myofibroblasts in the posterior corneal stroma at two to four months after keratitis (Figs. 2G, 2I, and 2K) are maintained by TGFβ that penetrated into the stroma from the aqueous humor. Thus, we hypothesize there is a critical role for Descemet's basement membrane in modulating TGFβ effects on keratocytes in the posterior cornea similar to the function of the EBM in modulating TGFβ and PDGF effects on keratocytes in the anterior stroma. This model provides an explanation for how posterior corneal fibrosis or haze could develop and persist following endothelial-Descemet's membrane damage, including fibrosis that is commonly noted as a complication of posterior lamellar surgical procedures such as Descemet's stripping automated endothelial keratoplasty and Descemet's membrane endothelial keratoplasty (Shulman et al., 2009; Kim et al., 2014). Since rabbit corneal endothelial cells can proliferate (Van Horn et al., 1977) it is possible that with longer follow-up beyond four months after keratitis the endothelium and Descemet's membrane could have regenerated across the central cornea, and posterior myofibroblasts would have undergone apoptosis. If so, the corneas would likely have become progressively less fibrotic and opaque, as has been noted in long-term studies of prior investigators (Hassell et al., 1983).

Acknowledgments

References

Abe R, Donnelly SC, Peng T, Bucala R, Metz CN. Peripheral blood fibrocytes: differentiation pathway and migration to wound sites. J. Immunol. 2001; 166:7556–62. [PubMed: 11390511]

Barbosa FL, Chaurasia SS, Cutler A, Asosingh K, Kaur H, Medeiros FW, Agrawal V, Wilson SE. Corneal myofibroblast generation from bone marrow-derived cells. Exp. Eye Res. 2010; 91:92–96. [PubMed: 20417632]

Bergers G, Song S. The role of pericytes in blood-vessel formation and maintenance. Neuro Oncol. 2005; 7:452–64. [PubMed: 16212810]

Cousins SW, McCabe MM, Danielpour D, Streilein JW. Identification of transforming growth factor-beta as an immunosuppressive factor in aqueous humor. Invest Ophthalmol Vis Sci. 1991; 32:2201–11. [PubMed: 2071334]

Fantes FE, Hanna KD, Waring GO, Pouliquen Y, Thompson KP, Savoldelli M. Wound healing after excimer laser keratomileusis (Photorefractive Keratectomy) in monkeys. Arch Ophthalmol. 1990; 108:665–75. [PubMed: 2334323]

Fleiszig SM, Evans DJ. The pathogenesis of bacterial keratitis: studies with Pseudomonas aeruginosa. Clin. Exp. Optom. 2002; 85:271–8. [PubMed: 12366347]

Gopinathan U, Sharma S, Garg P, Rao GN. Review of epidemiological features, microbiological diagnosis and treatment outcome of microbial keratitis: experience of over a decade. Indian J Ophthalmol. 2009; 57:273–279. [PubMed: 19574694]

Granstein RD, Staszewski R, Knisely TL, Zeira E, Nazareno R, Latina M, Albert DM. Aqueous humor contains transforming growth factor-beta and a small (less than 3500 daltons) inhibitor of thymocyte proliferation. J. Immunol. 1990; 144:3021–7. [PubMed: 2324494]

Hassell JR, Birk DE. The molecular basis of corneal transparency. Exp. Eye Res. 2010; 91:326–35. [PubMed: 20599432]

Hassell JR, Cintron C, Kublin C, Newsome DA. Proteoglycan changes during restoration of transparency in corneal scars. Arch Biochem Biophys. 1983; 222:362–9. [PubMed: 6847191]

Hazlett LD. Bacterial infections of the cornea (Pseudomonas aeruginosa). Chem. Immunol. Allergy. 2007; 92:185–94. [PubMed: 17264494]

Jester JV, Moller-Pederson T, Huang J, Sax CM, Kays WT, Cavangh HD, Petroll WM, Piatigorsky J. The cellular basis of corneal transparency: evidence for 'Corneal Crystallins'. J Cell Sci. 1999; 112:613–22. [PubMed: 9973596]

Kim K, Alder B, Vora GK, Carlson AN, Afshari NA, Kuo AN, Kim T. Textural interface opacity after Descemet-stripping automated endothelial keratoplasty. J Cataract Refract Surg. 2014; 40:1514–20. [PubMed: 25135544]

Ledbetter EC, Mun JJ, Kowbel D, Fleiszig SMJ. Pathogenic phenotype and genotype of Pseudomonas aeruginosa isolates from spontaneous canine ocular infections. Invest. Ophthalmol. Vis. Sci. 2009; 50:729–35. [PubMed: 18836164]

Marino GK, Santhiago MR, Santhanam A, Torricelli AAM, Wilson SE. Regeneration of defective epithelial basement membrane and restoration of corneal transparency. J Refract Surg. 2017 in press.

Marino GK, Santhiago MR, Torricelli AAM, Santhanam A, Wilson SE. Corneal molecular and cellular biology for the refractive surgeon: the critical role of the epithelial basement membrane. J Refract Surg. 2016; 32:118–25. [PubMed: 26856429]

Santhanam A, Marino GK, Torricelli AAM, Wilson SE. Epithelial basement membrane (EBM) regeneration and changes in EBM component mRNA expression in the anterior stroma after corneal injury. Mol Vis. 2017; 23:39–51. [PubMed: 28275314]

Shulman J, Kropinak M, Ritterband DC, Perry HD, Seedor JA, McCormick SA, Milman T. Failed descemet-stripping automated endothelial keratoplasty grafts: a clinicopathologic analysis. Am J Ophthalmol. 2009; 148:752–759. [PubMed: 19674726]

Singh V, Jaini R, Torricelli AAM, Santhiago MR, Singh N, Ambati BK, Wilson SE. TGFβ and PDGF-B signaling blockade inhibits myofibroblast development from both bone marrow-derived and keratocyte-derived precursor cells in vivo. Exp. Eye Res. 2014; 121:35–40. [PubMed: 24582892]

Singh V, Santhiago MR, Barbosa FL, Agrawal V, Ambati BK, Singh N, Wilson SE. Effect of TGFβ and PDGF-B blockade on corneal myofibroblast development in mice. Exp Eye Res. 2011; 93:810–7. [PubMed: 21978952]

Sta Iglesia DD, Stepp MA. Disruption of the basement membrane after corneal debridement. Invest Ophthalmol Vis Sci. 2000; 41:1045–53. [PubMed: 10752940]

Torricelli AAM, Singh V, Santhiago MR, Wilson SE. The corneal epithelial basement membrane: structure, function, and disease. Invest Ophthalmol Vis Sci. 2013a; 54:6390–6400. [PubMed: 24078382]

Torricelli AAM, Singh V, Agrawal V, Santhiago MR, Wilson SE. Transmission electron microscopy analysis of epithelial basement membrane repair in rabbit corneas with haze. Invest Ophthalmol Vis Sci. 2013b; 54:4026–33. [PubMed: 23696606]

Torricelli AAM, Santhanam A, Wu J, Singh V, Wilson SE. The corneal fibrosis response to epithelial-stromal injury. Exp. Eye Res. 2016; 142:110–18. [PubMed: 26675407]

Van Horn DL, Sendele DD, Siedeman S, Buco PJ. Regenerative capacity of the corneal endothelium in rabbit and cat. Invest Ophthalmol Vis Sci. 1977; 16:597–613. [PubMed: 873721]

Highlights

- Myofibroblast-mediated fibrosis causes scarring after microbial keratitis

- Defective epithelial basement membrane underlies myofibroblast development

- Epithelial basement membrane regeneration triggers myofibroblast disappearance
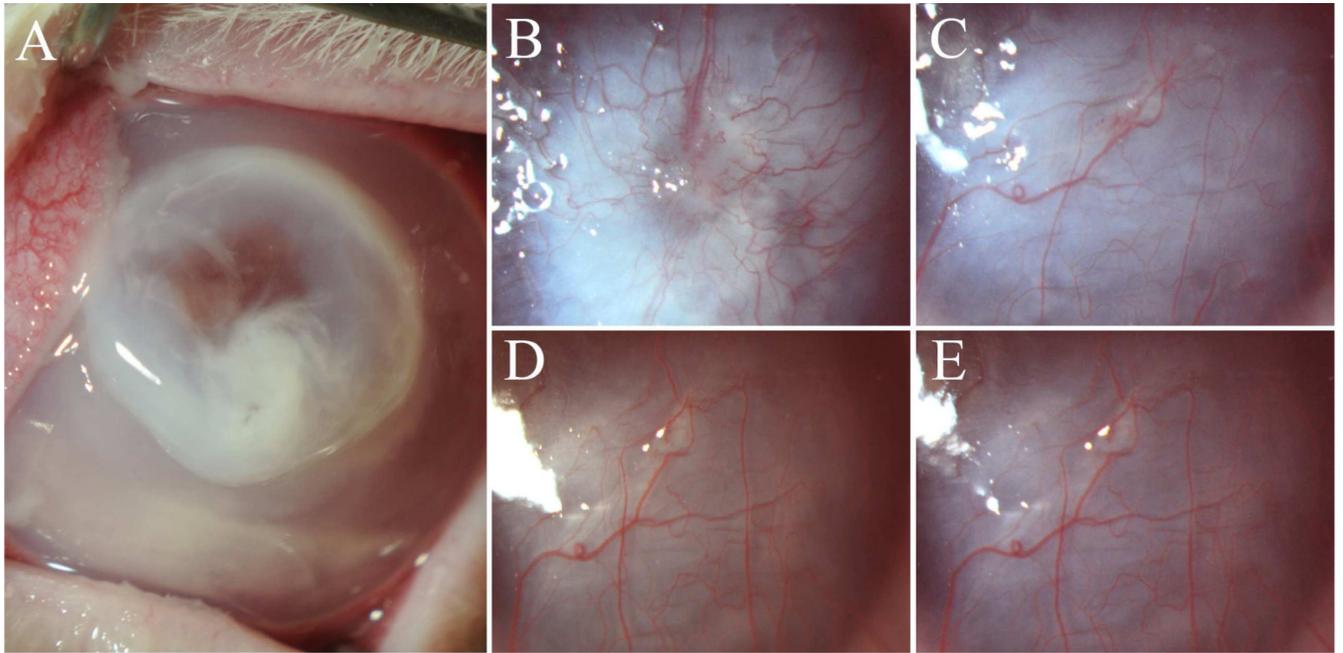
Fig. 1.
Slit lamp photographs of one of the rabbit corneas maintained for four months after keratitis at (A) 24 hours, (B) one month, (C) two months, (D) three months, and (E) four months after *Pseudomonas aeruginosa* keratitis. Note that scarring (fibrosis) is greatest at one month and decreased over several months, although iris details remain obscured at four months after keratitis. Vascularization of the stroma also occurred in all corneas by two months after keratitis. Mag. 20X.
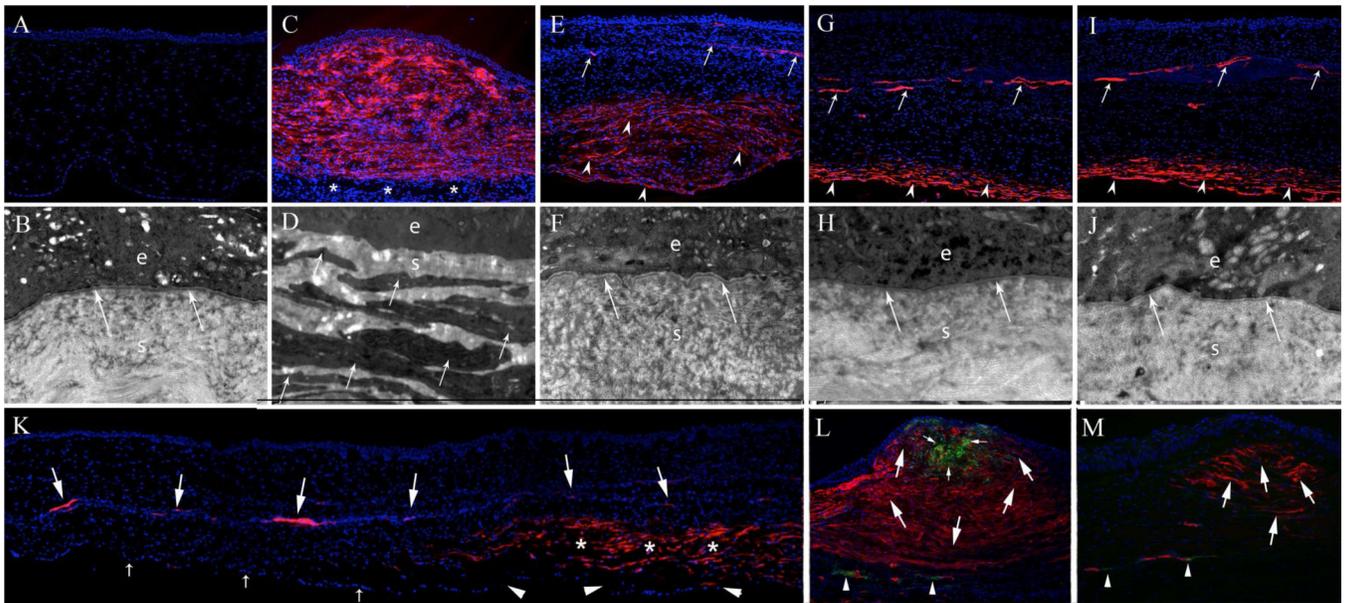
Fig. 2.
Immunohistochemistry (IHC) for alpha-smooth muscle actin and CD11b (200X mag.) and transmission electron microscopy (TEM) (23,000X mag.) of control unwounded corneas (A and B), and corneas at one month (C, D and L), two months (E, F and K), three months (G and H) and four months (I, J and M) after *Pseudomonas aeruginosa* keratitis. In a normal cornea (A and B) there are no α-SMA+ cells detected and normal EBM lamina lucida and lamina densa (arrows) are present beneath the epithelium (e). The underlying stroma (s) is populated with keratocytes. At one month after keratitis (C), the anterior stroma is filled with α-SMA+ cells that are primarily myofibroblasts. In this cornea, antibiotics halted the infection before the corneal endothelium was destroyed and the most posterior stroma is populated by α-SMA- keratocytes (*). TEM at one month after keratitis (D) found no detectible EBM beneath the epithelium (e) in all ten sections imaged. At one month after keratitis, the anterior stroma (s) is filled with large fibroblastic cells filled with rough endoplasmic reticulum that are the myofibroblasts (arrows). These are the α-SMA+ in IHC in panel C. At two months after keratitis (E), there are only a few α-SMA+ cells present in the anterior half of the stroma. Those α-SMA+ cells that persist in the anterior stroma (arrows) are likely pericytes associated with the invading blood vessels. Note that no corneal endothelial cells (α-SMA-) are present. In the TEM at two months after keratitis (F), EBM lamina lucida and lamina densa (arrows) are present beneath the epithelium (e). The myofibroblast cells that were present in the stroma (s) at one month after infection (D) are no longer seen at two months after infection (F). In IHC at three months after keratitis (G), almost all α-SMA+ myofibroblasts have disappeared in the anterior 80% to 90% of the stroma. The only α-SMA+ cells in the mid-stroma are associated with penetrating blood vessels (arrows). In the posterior 10% of the stroma α-SMA+ myofibroblasts (arrowheads) persist and no α-SMA- corneal endothelium is noted. In the TEM at three months after keratitis (H), normal lamina lucida and lamina densa (arrows) are noted beneath the epithelium (e) and no cells with large amounts of rough endoplasmic reticulum were present in the stroma (s). At four months after keratitis (I) α-SMA+ IHC is similar to that noted at

three months after infection. Again, in the posterior approximately 10% of the stroma α-SMA+ myofibroblasts (arrowheads) persist and no α-SMA- corneal endothelium is noted. In the TEM at four months after keratitis (J), normal EBM lamina lucida and lamina densa (arrows) are noted beneath the epithelium (e) and stroma (s). An IHC collage at two months after keratitis (K), shows a mid-peripheral area of the cornea where the corneal endothelium (small arrows) is intact and there are no overlying α-SMA+ cells in the posterior stroma. Conversely, in the adjacent more central area of the cornea the endothelium is damaged or absent (arrowheads) and the overlying stroma has layers of α-SMA+ myofibroblasts (*). A blood vessel that extends through the mid stroma has associated α-SMA+ cells (large arrows) that are likely pericytes. In a cornea at one month after keratitis in which double-IHC was performed for α-SMA and the monocyte lineage marker CD11b (Fig. 2L, and the same cornea shown in Fig. 2C) a localized nest of CD11b+ cells (small arrows) within the fibrotic stroma filled with α-SMA+ myofibroblasts (large arrows) likely represents a cluster of bone marrow-derived fibrocyte progenitors to myofibroblasts. Some CD11b antigen is also associated with neovascular blood vessels in the posterior stroma (arrowheads). In one four-month post-keratitis cornea, a localized pocket of persistent α-SMA+ myofibroblasts (arrows) was detected after performing serial sections (Fig. 2M) but no CD11b+ cells remained in the stroma at this time point, except for those associated with neovascular blood vessels (arrowheads). Presumably the EBM overlying this pocket remained defective, but this could not be confirmed since that portion of the cornea had been cryo-fixed and was not suitable for TEM analysis. All blue is DAPI staining of nuclei of all cells.